Beam Physics Note
TRI-BN-23-09
July 15, 2024

Approximate Jacobian for the Optimization Of Dipole Gap Profiles

Thomas Planche

TRIUMF

Abstract: I present here a formula to approximate the Jacobian matrix of a numerical root-finding problem I have often encountered: the iterative search, with a 3-dimensional finite element code such as OPERA, for the optimal gap profile of a dipole magnet. This formula is obtained from a particular 2-dimensional solution of Laplace's equation derived using conformal mapping. In this note, I focus on the derivation of the conformal mapping and I show how to compute the coefficients of the Jacobian matrix. I show a quick comparison with an `OPERA-3D` model at the end as a sanity check. I will present a full test case – the design of a cyclotron magnet where the pole shape is optimized using Newton's method – in a separate note.

1 Introduction

Consider the case of an iron-dominated dipole electro-magnet with a pole surface define by series of connected straight segment in, say, the radial direction, and with a constant height in the orthogonal (azimuthal) direction. To optimize the pole shape, i.e. the height of the end points of every straight segment, it would be useful the know how the magnetic field in the median plane is affected by an infinitesimal displacement of the end of every segment: this is the Jacobian matrix we are looking for.

To find a closed-form expression to calculate the coefficients of this matrix, let's simplify the problem a little. Let's reduce it to a 2-dimensional problem, and assume that the surface of the pole is an equipotential ($\mu_r \to \infty$). Let's also assume that the pole is locally approximately parallel to the median-plane: i.e. the variation of the gap height is small on the scale of 1 gap height.

Under these assumptions, the problem of knowing the effect of a small displacement of one point on the pole surface is reduced to calculate the field perturbation caused by a shallow triangular groove as illustrated in Fig. 1.

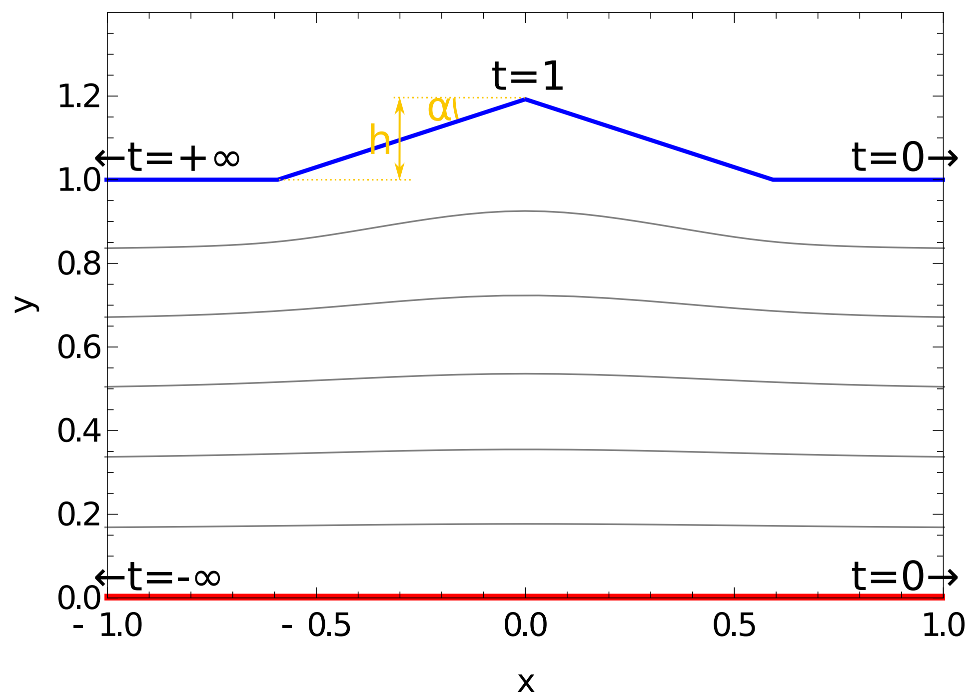

Figure 1: The blue line is the equipotential that goes along the pole surface; the red line is the equipotential that goes along the magnet midplane. A few more equipotentials, obtained from numerical integration of Eq. (2), are shown as thin grey lines. The values of t shown on the graph correspond to coordinates in the original space, see Section 2.

2 Conformal Mapping

Conformal mapping can be used to find analytical 2-dimensional solutions to Laplace's equation. The technique depends on constructing a transformation which preserves angles locally, from a geometry for which a solution is known, to the geometry of interest. A detailed introduction to the technique can be found in many E&M text books, see for instance [1, 2]. A couple of examples very similar to the case treated here can be found here [3].

Let x and y be the Cartesian coordinates of the geometry we are trying to solve for. If we construct two complex variables:

$$t = u + iv\,,\ \text{and}$$
$$z = x + iy\,,$$

the relation between them is given by the Schwarz-Christoffel formula:

$$\frac{\mathrm{d}z(t)}{\mathrm{d}t} = C\prod_n (t - t_n)^{\alpha_n/\pi - 1}\,, \tag{1}$$

where α_n is the internal angle of the n^{th} corner of the studied geometry, and t_n is the value of t associated with this corner in the in complex t-plane. The value of the constant $C \in \mathbb{C}$ is determined according to the specific scale of the problem. The magnetic field distribution is obtained from:

$$B(t) = B_x - iB_y = -\frac{\mathrm{d}\phi}{\mathrm{d}z} = -\frac{\mathrm{d}\phi}{\mathrm{d}t}\left(\frac{\mathrm{d}z}{\mathrm{d}t}\right)^{-1}\,. \tag{2}$$

The known solution we start from, $\phi(u, v)$, is that of the flat condenser:

$$\phi(u, v) = \frac{\Delta V}{\pi}\arctan\left(\frac{u}{v}\right) + V_0\,, \tag{3}$$

see [3, Fig.1]. The geometry we want to arrive at is the one shown in Fig. 1. This geometry possesses four corners (see Table 1).

t_n	α_n	z
0	0	$+\infty$
t_0	$\pi + \alpha$	$i - w$
1	$\pi - 2\alpha$	$i(1+h)$
t_1	$\pi + \alpha$	$i + w$

Table 1: Parameters of the four corners of the “transformed”geometry presented in Fig. 1. w is the half-width of the groove and h its depth.

Equation (1) thus becomes:

$$\frac{\mathrm{d}z}{\mathrm{d}t} = \frac{C}{t}(t - t_0)^a(t-1)^{-2a}\,(t - t_1)^a\,, \tag{4}$$

where $a = \alpha/\pi$. I choose to set $t_0 = 1/t_1$, which makes the groove left-right symmetrical.

We still need to choose the values of the constants C, ΔV and t_1. The value of C is chosen so that the magnitude of the magnetic field at $t = 0$ is 1 and pointing up, i.e. $B(0) = -i$, which leads to:

$$C = \frac{\Delta V}{\pi}\,. \tag{5}$$

ΔV is chosen so that the half-gap height outside the groove is 1, i.e. $\int_{-1}^{t_1}\frac{\mathrm{d}z}{\mathrm{d}t}\mathrm{d}t = i$, which leads to $\Delta V = -1$. The value of t_1 is related to the chosen value of the half-width w of the groove by:

$$2w = \int_{1/t_1}^{t_1}\frac{\mathrm{d}z}{\mathrm{d}t}\mathrm{d}t\,. \tag{6}$$

Since I don't know a closed-form expression for this integral, I will leave t_1 as a free parameter for now.

The resulting expression for the magnetic field is:

$$B(t) = -i \left(\frac{(t-1)^2 \; t_1}{(t-t_1) \; (t\, t_1 - 1)} \right)^a \, . \tag{7}$$

But what we really want is $B(z)$, and particularly $B_y(x)$, the field distribution along the median plane.

3 Closed-form expression in the limit of a shallow groove

When $a \to 0$ we can find an approximate expression for:

$$z(t) = \int_{-1}^{t} \frac{\mathrm{d}z}{\mathrm{d}t} \mathrm{d}t \approx \begin{cases} -\int_{-1}^{t} \frac{1}{\pi t} \mathrm{d}t, & \mathrm{Re}(t) < 0, \\ I - \int_{1}^{t} \frac{1}{\pi t} \mathrm{d}t, & \mathrm{Re}(t) > 0, \end{cases} = i - \frac{\ln t}{\pi} \, , \tag{8}$$

leading:

$$t(z) \approx -e^{-\pi z} \, . \tag{9}$$

With this approximation, we can express $B(t(z))$ with a closed-form expression, which along the median plane ($y = 0$) is:

$$B_y(x) = \left(\frac{2\, t_1 (\cosh(\pi x) + 1)}{t_1^2 + 2\, t_1 \cosh(\pi x) + 1} \right)^a \, . \tag{10}$$

The smaller is a, the better is the approximation, see Fig. 2.

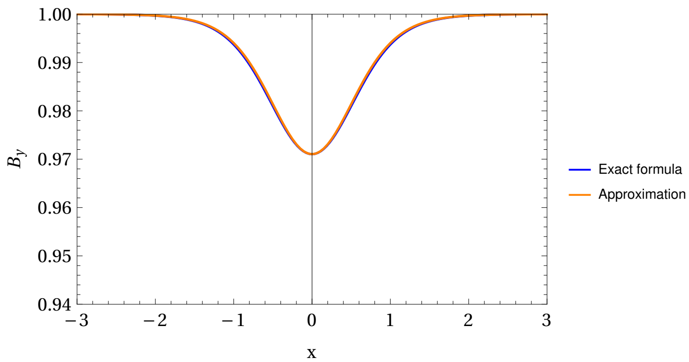

(a) $\alpha = \pi/20$, $t_1 = 5$

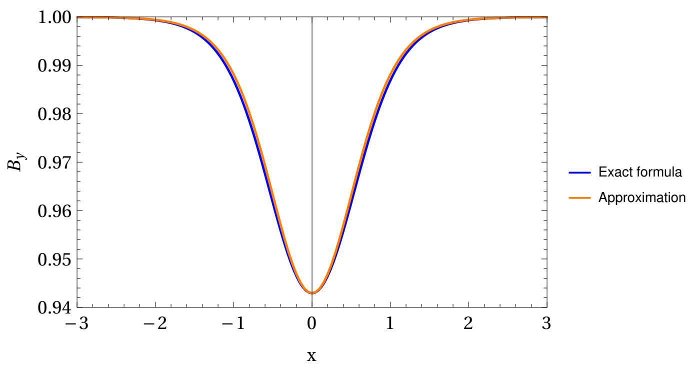

(b) $\alpha = \pi/10$, $t_1 = 5$

Figure 2: Magnetic field distribution $B_y(x)$ along the median plane ($y = 0$). The position x is given in unit of the magnet half-gap height. The numerical integration of the exact formula (blue) is compared with the approximate close-form formula (orange), for two different groove sizes, with the (a) case shallower than the (b) case. In the shallower case the two curves are virtually indistinguishable.

4 Jacobian matrix coefficient

What we really need is to express the relative effect of the groove as a function of the groove depth and width. From Eq. (10), using Eq. (8), we get along the median plane ($y = 0$) for $h \ll w$:

$$B_y(x) = \left(\frac{1 \qquad + \cosh(\pi x)}{\cosh(\pi w) + \cosh(\pi x)}\right)^{\frac{h}{\pi w}} . \tag{11}$$

Again, x is in unit of the half-gap height, and B_y is in unit of the magnitude of the field in the absence of a groove. In the limit where $h \to 0$:

$$B_y(x) \approx h \frac{\partial B_y(x)}{\partial h}\bigg|_{h=0} = \frac{h}{\pi w} \ln\left(\frac{1 \qquad + \cosh(\pi x)}{\cosh(\pi w) + \cosh(\pi x)}\right) . \tag{12}$$

The Jacobian matrix coefficient, expressed in units of the initial value per unit of the half-gap height, for a non-saturated magnet ($\mu_r \to \infty$), is:

$$\boxed{J_\infty(x) = \frac{1}{\pi w} \ln\left(\frac{1 \qquad + \cosh(\pi x)}{\cosh(\pi w) + \cosh(\pi x)}\right) .} \tag{13}$$

5 Verification of Equation 11 using OPERA-3D

I took the 3-dimensional model of a cyclotron sector magnet I am currently working on, and cut a small groove in the radial direction, see Figs. 3 and 4. The height of the groove is 5% of the half-gap height. I impose medial plane symmetry: this means that locally the magnet full gap height has been increased by 5%.

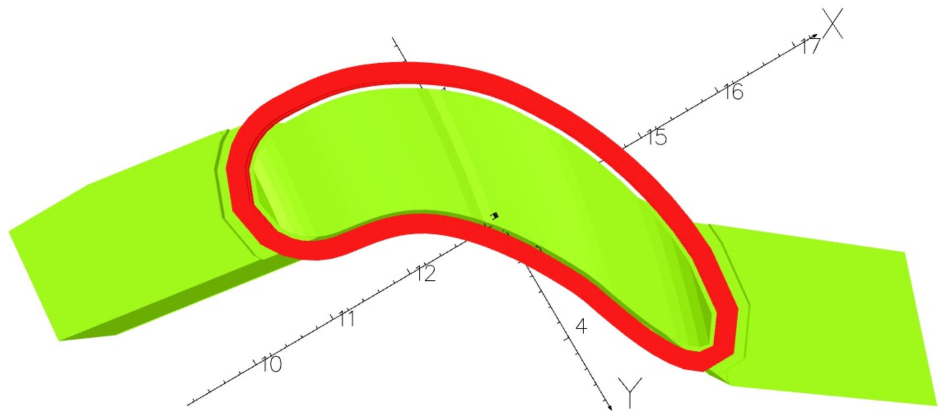

Figure 3: Top half of the cyclotron sector magnet used to test the conformal mapping result.

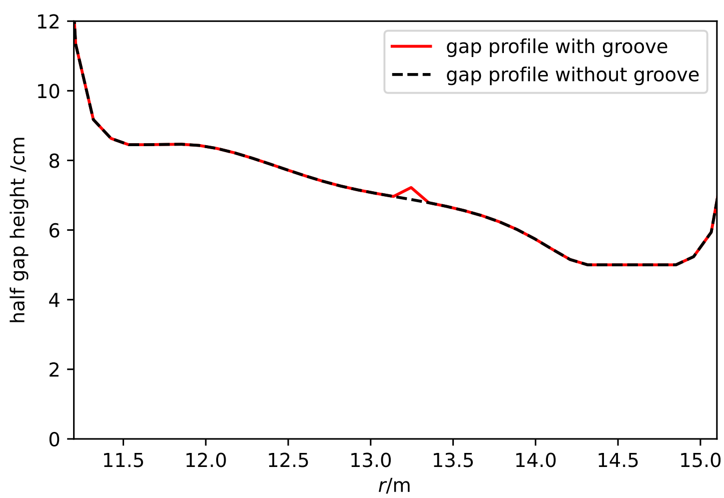

Figure 4: Radial pole profile of the magnet model shown in Fig. 3.

Far from magnetic saturation, the prediction form the conformal mapping model Eq. (11) is nearly perfect, see Fig. 5. Closer to magnetic saturation, the prediction is still close enough to be usable in a Newton–Raphson optimization, see Fig. 6. With a fully saturated magnet (I increased the coil current by a factor 5) the formula derived here is no-longer usable see Fig. 7.

There may be a way to modify this formula to make it somewhat usable for fully saturated magnets, by considering separately the direct contribution from the coil and the effect from the steel… but I will worry about that if the need ever comes to me to design such a magnet. For the present, this formula seems good enough for what I want to do. Let's put it to the test now. I will report the result of this test in a separate note.

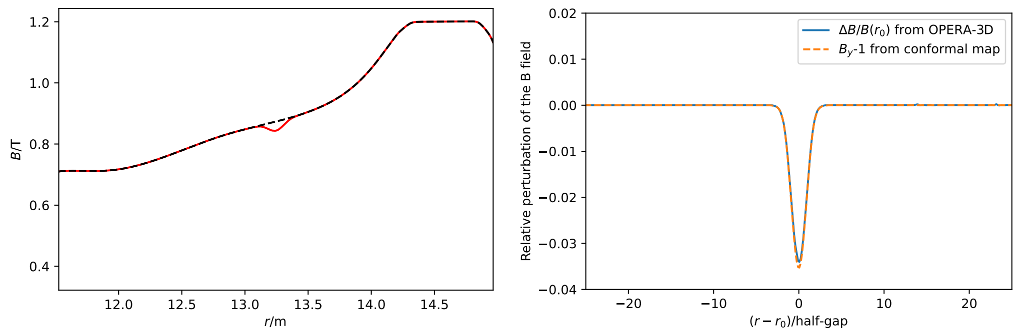

Figure 5: Test with with the magnet coils set at half of the nominal current. Left: magnetic field distribution along the center of the pole, in the magnet median plane, as a function of the machine radius r; the black dotted line is the initial field distribution, the red solid line is with the groove cut into the pole. Right: comparison between the field with and without the groove, normalized by 0.87 T, the initial magnitude of the magnetic field at the radius of the groove. Note that the horizontal axis on this graph is normalized by the half-gap height at $r = r_0$, which is about 6.9 cm, to allow direct comparison with Eq. (11).

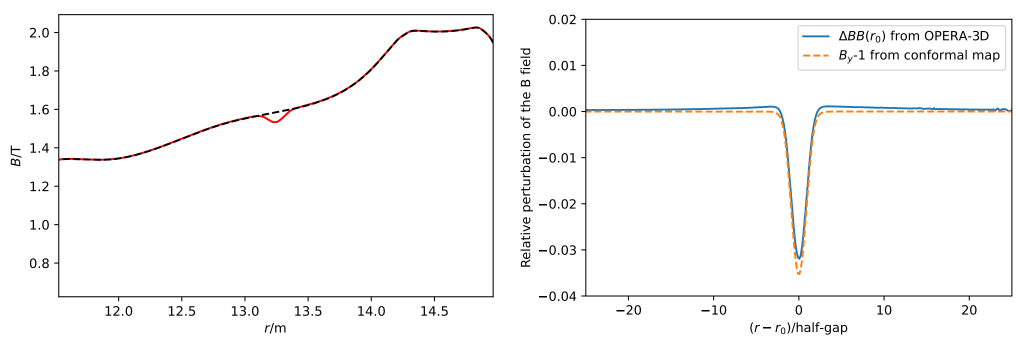

Figure 6: Same plots as in Fig. 5, but with the magnet coils set at the nominal current.

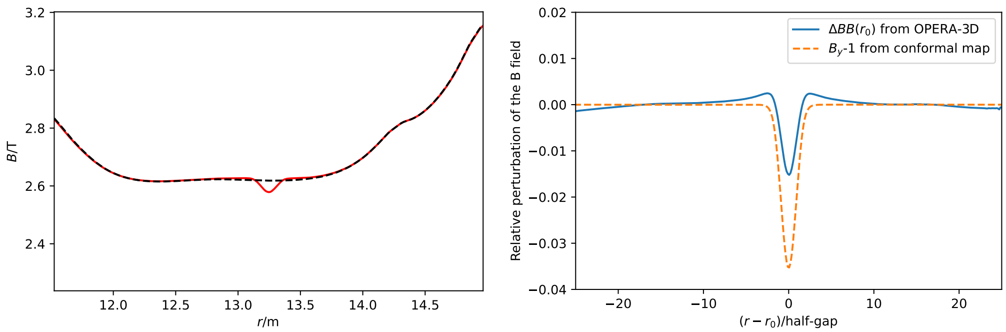

Figure 7: Same plots as in Fig. 5, but with a fully saturated magnet: the coils are set at five times the nominal current.

References

[1] E. Weber, Electromagnetic Fields: Theory and Applications, no. v. 1 in Electromagnetic Fields, Wiley, 1950.

[2] Z. Nehari, Conformal mapping, McGraw-Hill Book Company, Inc., 1952.

[3] T. Planche, P. M. Jung, S. Saminathan, R. Baartman, M. J. Basso, Conformal mapping approach to dipole shim design, Nuclear Instruments and Methods in Physics Research Section A: Accelerators, Spectrometers, Detectors and Associated Equipment 925 (2019) 101–105.